



## **Triboinformatics modelling of ultrahigh molecular weight polyethylene wear rate in total hip replacement using machine learning approaches**

Vipin Kumar, Ravi P. Tewari, Anubhav Rawat \*

Department of Applied mechanics, Moti Lal Nehru National Institute of Technology Allahabad Prayagraj U.P., INDIA.

\*Corresponding author: anubhav-r@mnnit.ac.in

---

### KEYWORDS

Machine learning  
Pin on disk test  
Total hip replacement  
UHMWPE  
Wear

---

### ABSTRACT

In current work, a relationship between ultrahigh molecular weight polyethylene wear rate and various parameters over which it depends on has been established using machine learning models for total hip replacement implants. Five machine learning based models, namely Artificial Neural Network, Random Forest, Support Vector Method, Gradient Boosting Machine and K nearest neighbor, are trained and tested using the experimental tribological dataset available in the literature to predict the wear rate. The R<sup>2</sup> ranged from 0.4 to 0.9, MSE has been found to be in the range of 3.89 to 15.65, RMSE varies in the range of 1.97 to 3.95, and MAE ranges from 1.02 to 4.87 for different ML approaches, which are remarkably small. Statistic based performance metrics also demonstrated that trained ML algorithms are able to predict UHMWPE wear rate for total hip replacement at a satisfactory level. Out of the five tested models KNN is found to perform best with the highest value of square of correlation coefficient i.e. 0.9 for the selected experimental dataset, indicating satisfactory performance of KNN model.

---

Received 17 June 2024; received in revised form 9 September 2024; accepted 13 September 2024.

To cite this article: Kumar et al., (2025). Triboinformatics modelling of ultrahigh molecular weight polyethylene wear rate in total hip replacement using machine learning approaches. Jurnal Tribologi 45, pp.82-103.

## NOMENCLATURE

P: Normal load [N]  
 A: Contact area [mm<sup>2</sup>]  
 f: Frequency [Hz]  
 S: Sliding distance per cycle [mm/C]  
 T: Lubricant temp. [°C]  
 C: Lubricant protein concentration [mg/ml]  
 Ra: Average disc surface roughness Ra [µm]  
 RD: Polyethylene radiation dose [kGy]  
 t: Test duration [MC]

## 1.0 INTRODUCTION

Total hip replacement (THR) is considered the most effective surgical procedure performed on individuals suffering from osteoarthritis and femoral necrosis. The number of primary THAs performed in the United States is expected to increase 175% by 2030 (Kenney, Dick, Lea, Liu, & Ebraheim, 2019). In hip replacement surgeries, the natural hip joint having deformity is replaced by an artificial implant, either metal on metal (MOM) or metal on polymer (MOP) type. In recent years, high metal ion levels, adverse local soft tissue reactions, carcinogenic effects, and high clinical failure have been observed MOM THR bearings (Levy & Ezzet, 2013). To overcome these shortcomings of MOM, MOP-type implants have been used for joint replacement implants and composed of metallic femoral heads coupled with polymer acetabular cups. The femoral head mainly comprises titanium or cobalt-chromium alloy. Generally, the medical purpose hip implants inserts are fabricated from Polyether-ether-ketone, high density polyethylene and ultrahigh molecular weight polyethylene (UHMWPE). Currently UHMWPE is one of these recently available important materials which improve hip implants life substantially. Though the life span of THR implants is considered to be high but the failure of the acetabular cup is still a matter of concern. As the time span of THR surgery progresses, the artificial joint starts to produce wear particles at the micro and nanoscale due to mechanical and biological interaction between the replaced joint surfaces. These wear particles may initialize inflammatory tissue response resulting from macrophages, leading to osteolysis. The infiltrated and resident macrophages, neutrophils, and fibroblasts are activated by the joint implants wear particulates at the implant site. Neutrophils recognize biomaterials and form neutrophil extracellular traps (NETs). Fibroblasts and macrophages are involved in leukocyte recruitment at the prosthesis interface. The tumor necrosis factor (TNF- $\alpha$ ) and IL-1 facilitate inflammatory response and, combined with RANKL, can give rise to osteoclast precursor cells differentiation into activated bone-resorbing cells (Couto et al., 2020). This macrophage induced osteolysis leads to bone resorption at the bone and implant interface, and hence implant loosening happens. Due to osteolysis, the pace of bone formation is observed to be lower than bone resorption, resulting in bone volume loss (Shen, Fang, & Kang, 2018).

The implant loosening phenomenon could possibly decrease the life span of THR prosthesis and thus affect the quality of life, joint function, and mobility. Researchers from all over the globe have used multiple strategies to improve resistance against wear and mechanical properties by modifying processing steps, crosslinking heat treatment, and antioxidant addition. Various research works available in the literature are mainly focused on improving the mechanical and

tribological properties of UHMWPE cups. Pin on disk (POD) has been extensively used in quantifying and comparing the wear performance of different material combinations based on their operating parameter and ambience conditions (A Borjali, Monson, & Raeymaekers, 2019). The POD testing apparatus includes a pin that is pressed against a rotating disk, and relative motion between them results in the UHMWPE wear. The effect of cross-shear was observed on the pin surface in circular and elliptical wear trajectories, whereas in rectangular and square wear paths, the cross-shear was seen when the pin changed its direction along the wear path.

The serum types and their operating temperatures also play a significant role in the wear and friction phenomenon of UHMWPE in multi-directional testing (Saikko, Morad, & Viitala, 2022). Alpha calf serum (ACS) and bovine calf serum (BCS) are the most commonly used lubricants for tribological testing due to their stability against heat and denaturation. Recent developments, involving vitamin E blending in UHMWPE, show superior oxidative and wear resistance. Several studies have reported that UHMWPE wear depends on BCS protein concentration, protein type, and temperature (Saikko, Morad, & Viitala, 2021). The UHMWPE wear is also dependent on crosslinking of polyethylene and the surface roughness of the rotating disk surface. Crosslinking is achieved mainly through irradiation. As it can be seen, the tribological performance of UHMWPE is dependent on various features. It is somewhat difficult to evaluate the wear rate for each feature by POD-based studies in time.

Wear and friction phenomenon of UHMWPE in multi-directional testing (Saikko et al., 2022). Alpha calf serum (ACS) and bovine calf serum (BCS) are the most commonly used lubricants for tribological testing due to their stability against heat and denaturation. Recent developments, involving vitamin E blending in UHMWPE, show superior oxidative and wear resistance. Several studies have reported that UHMWPE wear depends on BCS protein concentration, protein type, and temperature (Saikko et al., 2021). The UHMWPE wear is also dependent on crosslinking of polyethylene and the surface roughness of the rotating disk surface. Crosslinking is achieved mainly through irradiation. As it can be seen, the tribological performance of UHMWPE is dependent on various features. It is somewhat difficult to evaluate the wear rate for each feature by POD-based studies in time.

POD-based wear studies are time-consuming and very expensive. The researchers are concentrated on in-silico studies and are proven to be an alternative to these POD-based wear testing. However, in-silico studies could not replace these POD-based testing completely but can give insight into experimental wear evaluation and have applications in biomedicine biomechanics and tribology. Since in-silico investigations require well-defined mathematical models or expression, limiting their prediction ability due to non availability of mathematical ones. The unavailability of mathematical models is the most critical problem in tribological investigations.

The rise of artificial intelligence and machine learning (ML) have shown their superiority in modeling complex relationships among various attributes, which is impossible in traditional parametric studies. ML based approaches viz. Artificial Neural Networks, K-Nearest Neighbor, Gradient Boosting Machine, and Random Forests employ advanced algorithms to find complex relationship in data and predict the target variable precisely. Such kind of data driven models have been precisely applied to predict the flow characteristics in pipes (Sethi, Rawat, Srivastava, & Sharma, 2022), air pollution level (Pandey, Kumar, Rawat, & Rawal, 2023), and wear and friction of aluminum alloys from tribological test conditions. Machine learning can also be applied to optimize the hip implant design from plain radiographs (Alireza Borjali, Chen, Muratoglu, Morid, & Varadarajan, 2020), detection of implant loosening (Shah, Bini, Martinez, Padoia, & Vail,

2020), identification of femoral stems (Kang, Yoo, Cha, Park, & Kim, 2020), and predict the post-operative outcomes (Bini et al., 2019). The experimental studies based on POD trials play a crucial role in assessing the wear performance of these hip implants. The results obtained from the research carried out by different research groups vary greatly; hence, it is challenging to compare the results, leading to a potential information gap. The above cited data-driven algorithms have the potential to fill this gap and establish a relationship between the variable, which is very difficult in experimental studies.

The above literature survey reveals that the applicability of machine learning models in the prediction of UHMWPE wear rate is very limited and hardly any work has been reported so far that utilizes an experimental dataset in the context of total hip replacement implants. Traditionally, friction and wear phenomena have been observed by varying one or two parameters simultaneously. It is often difficult to generate a universal understanding of friction and wear due to the complexity of the parameters defining them. This problem can be solved using machine learning algorithms since these algorithms are a promising solution to dealing with tribological data's inherent complexity. Thus, in the current work, a suitable experimental data from the literature has been chosen which involves Contact area [mm<sup>2</sup>], Normal load [N], Wear path shape Frequency [Hz], Average disc surface roughness Ra [μm], Lubricant temperature [°C], Wear path aspect ratio, Sliding distance per cycle [mm/C], Lubricant protein concentration [mg/ml], Test duration [MC], and Polyethylene radiation dose [kGy], and use it to train various suitable machine learning models to find the optimum one.

## 2.0 MATERIALS AND METHODS

### 2.1 Details of Selected Experimental Data

A comprehensive dataset, encompassing all input and target attributes, is essential for developing an effective machine learning model. The process of acquiring the dataset is crucial, as the predictive performance of the machine learning model heavily depends on the quality and relevance of the dataset. It is time and cost consuming to perform in-vitro studies for the dataset, which are based on the multi-directional pin on disk wear experiments. Due to these possibilities, an exhaustive literature survey is performed targeting critical technical aspects (Baykal et al., 2014; Bistolfi & Bellare, 2011; A Borjali et al., 2019; Bragdon et al., 2001; Greenbaum, Burroughs, Harris, & Muratoglu, 2004; Gul, McGarry, Bragdon, Muratoglu, & Harris, 2003; Harsha & Joyce, 2013; Hunt & Joyce, 2016; Korduba & Wang, 2011; Kurtz, MacDonald, Kocagöz, Tohfafarosh, & Baykal, 2014; Langhorn, Borjali, Hippensteel, Nelson, & Raeymaekers, 2018; Laraia, Leone, MacDonald, & Blanchet, 2006; Mazzucco & Spector, 2003; Muratoglu et al., 2003; Nakanishi et al., 2018; Oral, Neils, & Muratoglu, 2015; Oral, Wannomae, Hawkins, Harris, & Muratoglu, 2004; Saikko, 2017; Saikko, Calonius, & Keränen, 2001, 2004; Sawae, Yamamoto, & Murakami, 2008; Turell, Wang, & Bellare, 2003; Wimmer, Sah, Laurent, & Viridi, 2013; Yao, Blanchet, Murphy, & Laurent, 2003). The literature survey manifested and established the importance of “wear”, “tribological performance”, “pin-on-disc/disk”, “hip joint replacement”, “UHMWPE”, “Co-Cr”, “Co-Cr-Mo” and “Crosslinking”, “surface roughness”, “highly crosslinked polyethylene” for accumulating the UHMWPE wear rate dataset generated due to Co-Cr alloy (Baykal et al., 2014; Bistolfi & Bellare, 2011; A Borjali et al., 2019; Bragdon et al., 2001; Greenbaum et al., 2004; Gul et al., 2003; Harsha & Joyce, 2013; Hunt & Joyce, 2016; Korduba & Wang, 2011; Kurtz et al., 2014; Langhorn et al., 2018; Laraia et al., 2006; Mazzucco & Spector, 2003; Muratoglu et al., 2003;

Nakanishi et al., 2018; Oral et al., 2015; Oral et al., 2004; Saikko, 2017; Saikko et al., 2001, 2004; Sawae et al., 2008; Turell et al., 2003; Wimmer et al., 2013; Yao et al., 2003).

The dataset for this study was taken from the supplementary data provided by borjali et al. (A Borjali et al., 2019). The year wise distribution of investigated literature is given in Figure 1.

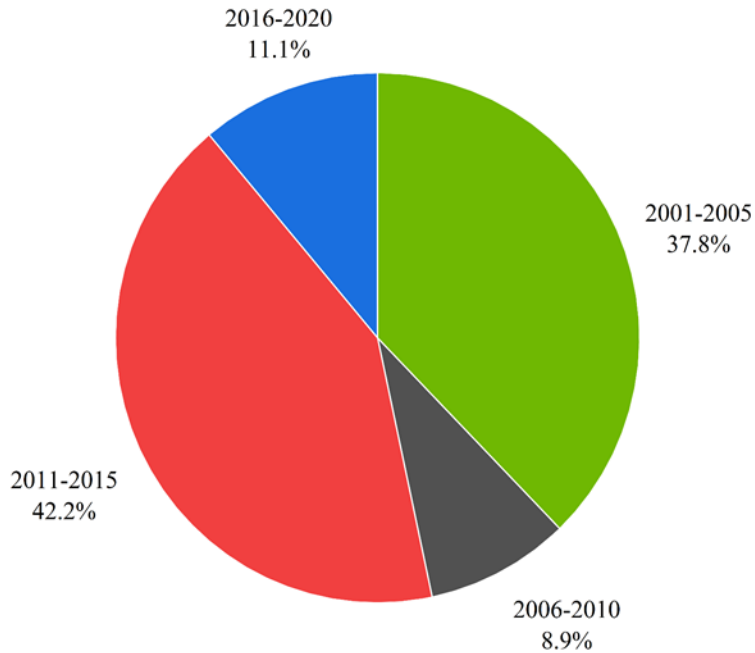


Figure 1: Year wise percentage distribution of the investigated literature.

The detailed statistical analysis of whole UHMWPE dataset containing 129 instances is given in Table 1. The Table 1 contains the minimum, maximum, mean and standard deviation of whole dataset. As mentioned earlier, the literature reveals that the UHMWPE wear rate depends on input features like Contact area, Normal load, Wear path shape, frequency, and average disc surface roughness. The detailed statistical analysis of the whole UHMWPE dataset containing instances is given in Table 1, and a graphical representation of the characteristics of each input variable is shown in Figure 2. The contact area has a wide range with a maximum value greater than its average value (Table 1). Similar to the Contact area, Normal load values are also greater than its mean values. Frequency values are concentrated around average value with a relatively small standard deviation. The surface roughness parameter has a limited range, and its mean is found to be close to its standard deviation. The temperature parameter is found to be spread out and shows a significant difference between maximum and minimum values. The lubricant protein concentration and test duration data are found to be right skewed, having maximum values greater than their mean value. The data imputation technique is applied to deal with missing values in each row in which NaN values are present. The missing values of each input attribute are replaced by their respective mean, which is very common practice while training machine learning based models. In the dataset, wear path shape is considered as categorical value which is transformed into numerical values by applying label encoding. Before training the machine

learning models, circular, elliptical, square, and rectangular wear paths are encoded as 1, 2, 3, and 4 respectively.

Table 1: Descriptive statistics of UHMWPE wear rate data (A Borjali et al., 2019).

<b>Input Features</b>	<b>Max</b>	<b>Min</b>	<b>Missing values</b>	<b>Average</b>	<b>Standard deviation</b>
Contact area [mm <sup>2</sup> ]	706.86	7.07	0	67.15	67.11
Normal load [N]	777.55	7	0	166.26	129.38
Wear path shape	Circular with diameter d = 10 mm	Rectangular with dimension 10 × 20 mm	0	-	-
Frequency [Hz]	2	0.2	0	1.25	0.43
Average disc surface roughness Ra [μm]	0.50	0.001	4	0.05	0.10
Lubricant temp. [°C]	37	20	63	29.23	7.50
Wear path aspect ratio	10.98	1	0	1.79	1.58
Sliding distance per cycle [mm/C]	94.25	17.76	0	30.47	10.08
Lubricant protein concentration [mg/ml]	64.8	0.69	33	22.28	6.35
Test duration [MC]	3.2	0.1	0	2.02	0.93
Polyethylene radiation dose [kGy]	150	0	0	36.31	40.77
Polyethylene wear rate [mg/MC]	34.62	0.00	0	5.73	6.36

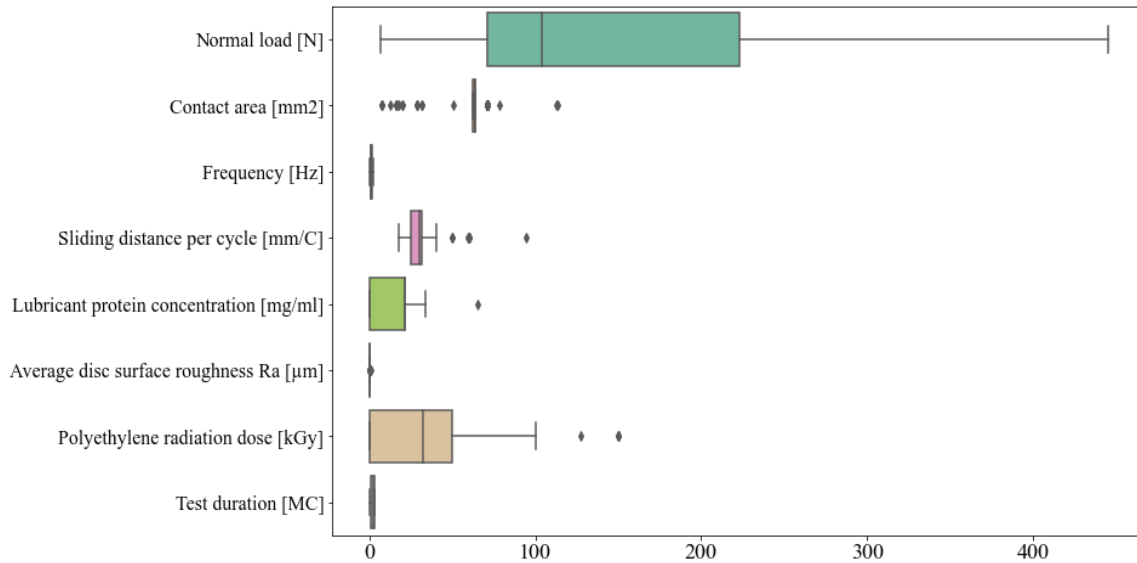


Figure 2: Box plot representing the characteristics of each input parameter.

## 2.2 Machine Learning Models

In this current study, supervised machine learning based models viz. Artificial Neural Network (ANN), Random Forest (RF), Support Vector Method (SVM), Gradient Boosting Machine (GBM), and K nearest neighbor (KNN), were trained and tested with the data extracted from literature to establish a relationship between input attributes and UHMWPE wear rate. The selection of machine learning algorithms is solely based on their suitability and capability for the problem being addressed. ANN can handle non-linear relationships and complex patterns, making it a popular choice for data analysis. Furthermore, Random Forest (RF) is employed to minimize overfitting and be robust against the noisy data. Both linear and non-linear data can be handled using SVM. Using GBM, multiple weak models are built sequentially to correct errors made by previous models. It handles missing data well and excels at handling complicated relationships between features. Lastly, the KNN model can be utilized when the distribution of the dataset is unknown.

The general pipeline for training and testing of ML model has been shown in Figure 3. Basically, ANN is a computer algorithm that processes the information like human brain does naturally and have the potential to solve complex problems which are very difficult to solve by traditional approaches. ANN network comprises inter-connected neurons, forming a structure analogous to the human brain. The fully trained ANN model can create useful outputs for fresh datasets based on its learning experiences. Each ANN has an input layer with nodes equal to the number of independent variables known as input variables and an output layer with neurons equal to the number of output variables. The layers between the input and output layers are commonly referred to as hidden layers. The functional unit of ANNs is the neuron or node, and they are linked together by a weight factor. The sum of input variables to weights is transformed into an output value in each neuron using an activation function. The sigmoid activation and Tanh are the most commonly used activation functions for input and hidden layers, and the linear

activation function is generally used for the output layer. The mathematical expression of sigmoid activation has been given by Equation (1).

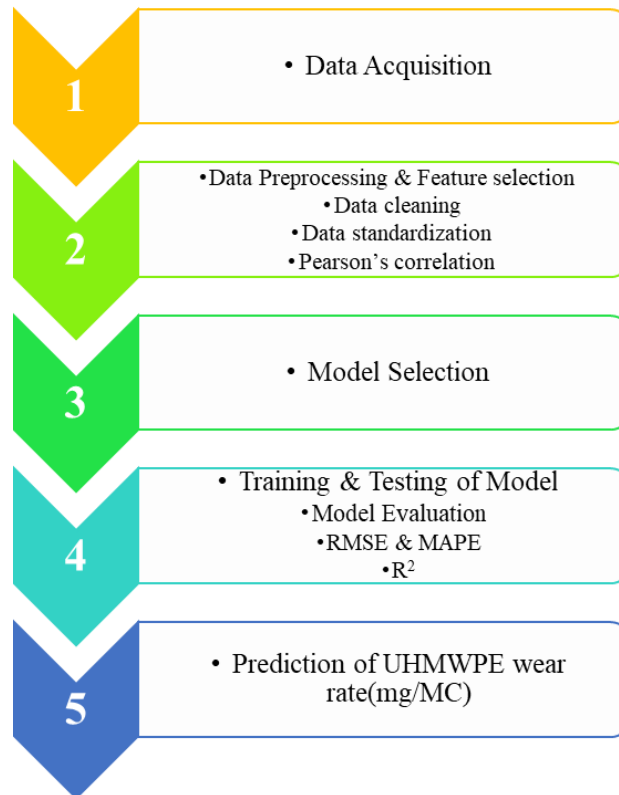


Figure 3: A typical machine learning pipeline containing all the steps which are explained in section.

$$A = \frac{1}{1 + e^{-z}}, \quad \text{and} \quad z = wx + b \quad (1)$$

Tanh activation function mathematically has been described in Equation 2.

$$f(x) = \frac{2}{(1 + e^{-2x})} - 1 \quad (2)$$

Random Forest is a machine learning technique that learns and develops from training data using decision trees. This approach is well-known for handling large data and modeling more sophisticated co-relationship using multiple input attributes. The outcomes of decision trees are accumulated, giving RF better forecasting abilities. Overfitting to training instances in simple decision trees can be eliminated using RF techniques. The RF approach starts by considering various bootstrap samples, which have been taken at random from training data, and these bootstrap samples are fitted with regression trees. The binary partitioning has been performed

by considering a tiny set of input attributes for each node per tree randomly chosen from the total dataset.

The final prediction is obtained by averaging the predictions of all the trees in the forest.

$$\bar{y} = \frac{1}{N} \sum_{i=1}^N \{y(x, \theta_i)\} \quad (3)$$

Where,  $\bar{y}$ ,  $x$  represents the model prediction, independent variable, while  $\theta$  is an identically distributed random vector, and  $h(x, \theta)$  is the output calculated based on  $x$ .

The prediction of any observation in RF model is evaluated by calculating the mean of all the trees. RF frequently beats most other ML methods due to this distinguishing feature. Several critical parameters viz. the max features and n\_estimators must be optimized in order to maximize the performance of RF models.

Kernelized SVM is a supervised machine learning technique that excels at managing a large number of input attributes with a small dataset. SVM regression techniques need rearranging data points into hyper-planes in higher dimensional space. Various kernel functions are available for organizing data points into higher dimensional hyper-planes. The SVM model complexity and quality are controlled by SVM meta-parameters, loss function ( $\epsilon$ ), and error penalty factor (C). In addition, the selection of the kernel function has an important impact on the final models. The radial basis kernel function (RBF) is commonly used in the SVM regression approach. These parameters must be adjusted together to improve model performance.

The mathematical expression for the RBF function is given by Equation (4):

$$K(x, x') = \exp\left(\frac{\|x - x'\|}{2\sigma^2}\right) \quad (4)$$

where  $x, x'$  are vector points in any fixed dimensional space.

The ensemble approach, which combines many decision trees, is used to generate the GBM prediction model. Every tree in the GBM model analyses a specific data segment and optimizes loss functions for each tree. The outcomes of every tree are then integrated to provide an accurate forecast. The intricacy of the GBM approach is defined by learning rate and n\_estimators. The simultaneous modification of these parameters corroborates that the model is optimized.

The boosting algorithm grows the decision trees by minimizing the following objective function:

$$\Phi = \sum_i l(y_i', y_i) \quad (5)$$

where  $l$  is the loss function that measures the mean squared error between the prediction  $y'$  and the actual value  $y$ .

KNN evaluates the nearest neighbors in the training dataset to forecast unknown data. Due to the fact that the KNN approach does not utilize a training dataset for generalization, it is also known as a lazy algorithm. In this approach, the nearest neighbors are weighted inversely by their centre distance. In the KNN regression model, the same distance function is used as in the case of the KNN classification model. The functions which describe how the distance is measured

between two data points, Euclidian (ED) and Manhattan distance (MD), are given by Equation (6) and Equation (7) respectively.

$$E_D = \sqrt{\sum_{i=1}^k (x_i - y_i)^2} \quad (6)$$

$$M_D = \sum_{i=1}^k |x_i - y_i| \quad (7)$$

The final prediction in the KNN model has been calculated on the basis of the average of k-nearest neighbors' predictions as given by Equation (8).

$$\hat{y} = \frac{1}{k} \sum_{i=1}^k y_i(X) \quad (8)$$

The parameter "k" represents the number of neighbours evaluated in the forecasting of an unknown data. The complexity of a KNN model is defined by the value of k. As a result, for speed optimization, k must be carefully chosen based on the dataset and the intricacy of the task.

### 2.3 Feature Selection and Pre-Processing

To ensure the accuracy and reliability of ML models' predictions, several key pre-processing steps are performed. First, missing data is handled by employing appropriate imputation techniques to fill in missing values by their mean values, ensuring a complete dataset for analysis. Next, the data is normalized to bring all input features onto a similar scale, which is particularly important for machine learning models that are sensitive to the magnitude of the data, such as K-Nearest Neighbors (KNN) and Support Vector Machines (SVM). Additionally, feature selection is performed by using Pearson correlation coefficient to identify and retain only the most relevant attributes, reducing noise and improving model performance. These pre-processing steps are crucial in preparing the dataset, enabling the machine learning models to make accurate and robust predictions of the wear rate in UHMWPE hip replacement implants. The Pearson correlation function is established between the features and labels. This correlation coefficient determines the relative importance of each feature to the labels. The heat map diagram is used to express the variance across all training features and to observe the correlation among all of the features. The heat map diagram has been shown in Figure 4.

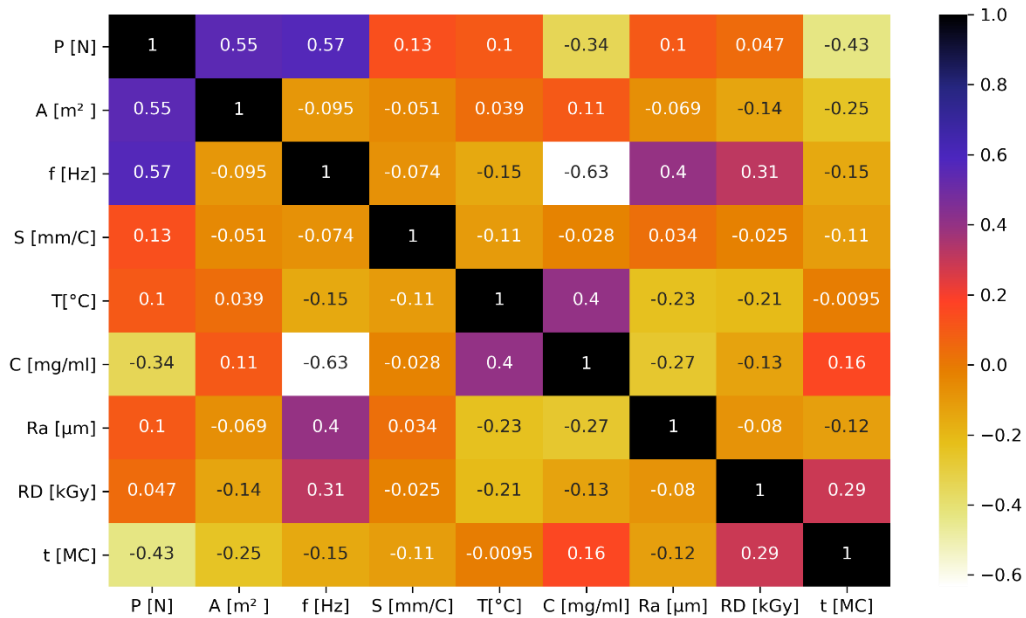


Figure 4. Heatmap displaying the relationship between the training features of the dataset.

It can be observed from Figure 4 that there is no strong co-relationship between the input attributes as their ‘Pearson correlation coefficient’ values are less than 0.9. The Pearson correlation coefficient is denoted as  $r$  and ranges from -1 to 1. A value of 1 indicates a perfect positive linear relationship, -1 indicates a perfect negative linear relationship, and 0 indicates no linear relationship between the variables. A Pearson correlation heatmap helps to avoid collinearity or duplicity between variables by visually displaying the strength of linear relationships between pairs of variables. High correlation values, indicated by distinct colors in the heatmap, signal that two variables are strongly related and may contain redundant information. By identifying these highly correlated variables, the heatmap allows to make informed decisions about which variables to exclude from the analysis, thereby reducing multicollinearity. This process improves the stability, accuracy, and interpretability of a statistical or machine learning model by ensuring that the variables included are more independent and contribute unique information. All available independent parameters, as mentioned in Table 1 on which UHMWPE wear rate is dependent, are used for training and testing ML based models. The ten-fold cross-validation was applied to compute the error in the prediction of polyethylene wear using ML models. The dataset is randomly divided into  $n$  number of equal subsets, called folds. Then,  $n-1$  subsets are used to train the ML based models, and one remaining subset is used for cross-validation of that model. This procedure was repeated  $n$  times to make it possible for the model to be validated for each subset of data at least once. In cross-validation, the model was validated with the dataset that was not part of the model training.

## 2.4 Model Performance Criteria

The model performance can be evaluated using a variety of metrics, including the mean absolute error (MAE), root mean square error (RMSE), and the square of the correlation coefficient (R2), which have been briefly explained in the subsequent section (Srivastava, Prakash, & Rawat, 2022).

### Mean absolute error

$$MAE = \frac{\sum_{i=1}^n |o_a - o_p|}{n} \quad (9)$$

Where  $o_a$  and  $o_p$  are the true and forecasted values of the  $i$ th instance and  $n$  represents the total number of instances in the data.

### Root mean square error

$$RMSE = \sqrt{\frac{\sum_{i=1}^n (o_a - o_p)^2}{n}} \quad (10)$$

### Square of the correlation coefficient

$$R^2 = 1 - \frac{\sum_{i=1}^n (o_a - o_p)^2}{\sum_{i=1}^n (o_a - \bar{o}_a)^2} \quad (11)$$

## 3.0 RESULTS AND DISCUSSION

As described earlier, in this section, the results obtained using various ML models shall be discussed and compared with each other to establish the best possible ML model for the prediction of hip joint wear accurately.

### 3.1 Parameter Optimization of ML Based Models

Parameter optimization is a technique for improving the performance of machine learning algorithms. To find the best parameters for the ML approaches in Tables 2 and 3, the grid search method is used. Different parameter ranges are defined, and the grid search approach is made to perform multiple ML analyses using various combinations of these parameters. The grid search approach recommends parameters that generates the optimum results by comparing model performance for different combinations of parameters. The hyperparameter with search space and optimized results of parameter tuning ML algorithms for UHMWPE wear rate predictions are represented in Table 2.

Table 2: Optimized parameter of ML based models for UHMWPE wear rate.

Machine learning model	Optimized parameter
ANN	Hidden layer sizes = (15,15,15), alpha = 0.01, activation function: "sigmoid"
GBM	n_estimator = 10, learning rate = 0.3
SVM	kernel = "rbf", C = 20, gamma = 0.8
KNN	n = 3, weight = "distance", p=2
RF	n_estimators = 10, max_features = 2

### 3.2 Model Performance Evaluation

In the current work, five ML models, namely ANN, RF model, SVM, GBM and KNN, are used. The square of correlation coefficient ( $R^2$ ) is the most commonly used metric while evaluating the performance of these regression-based ML models. The  $R^2$  indicates the percentage of variance in data described by the regression method. Aside from  $R^2$ , MAE, MSE, and RMSE are also important measures for evaluating model performance. The performance metrics for each ML model used in the current study are evaluated and summarized in Table 3. It is evident from Table 3 that the values of  $R^2$  on the testing dataset ranged from 0.4 to 0.9 for different ML models. It can also be observed from the Table 3 that MSE has been found to be in the range of 3.89 to 15.65, RMSE varies in the range of 1.97 to 3.95, and MAE ranges from 1.02 to 4.87 for different ML approaches, which are remarkably small. Statistic based performance metrics also demonstrated that trained ML algorithms are able to predict UHMWPE wear rate at a satisfactory level.

Table 3. Wear rate analysis using machine learning methods for UHMWPE.

Machine learning Model	Mean squared error (MSE)	Mean absolute error (MAE)	Root mean squared error (RMSE)	$R^2$ value
ANN	6.86	2.24	2.61	0.65
RF	13.02	2.14	3.60	0.68
SVM	15.65	4.87	3.95	0.4
GBM	4.35	1.86	2.08	0.65
KNN	3.89	1.97	1.02	0.9

A detailed comparison of predicted values obtained from RF, GBM, SVM, ANN based regression models and actual values of wear rate of UHMWPE acetabular cup for hip joint replacement has been shown in Figure 5.

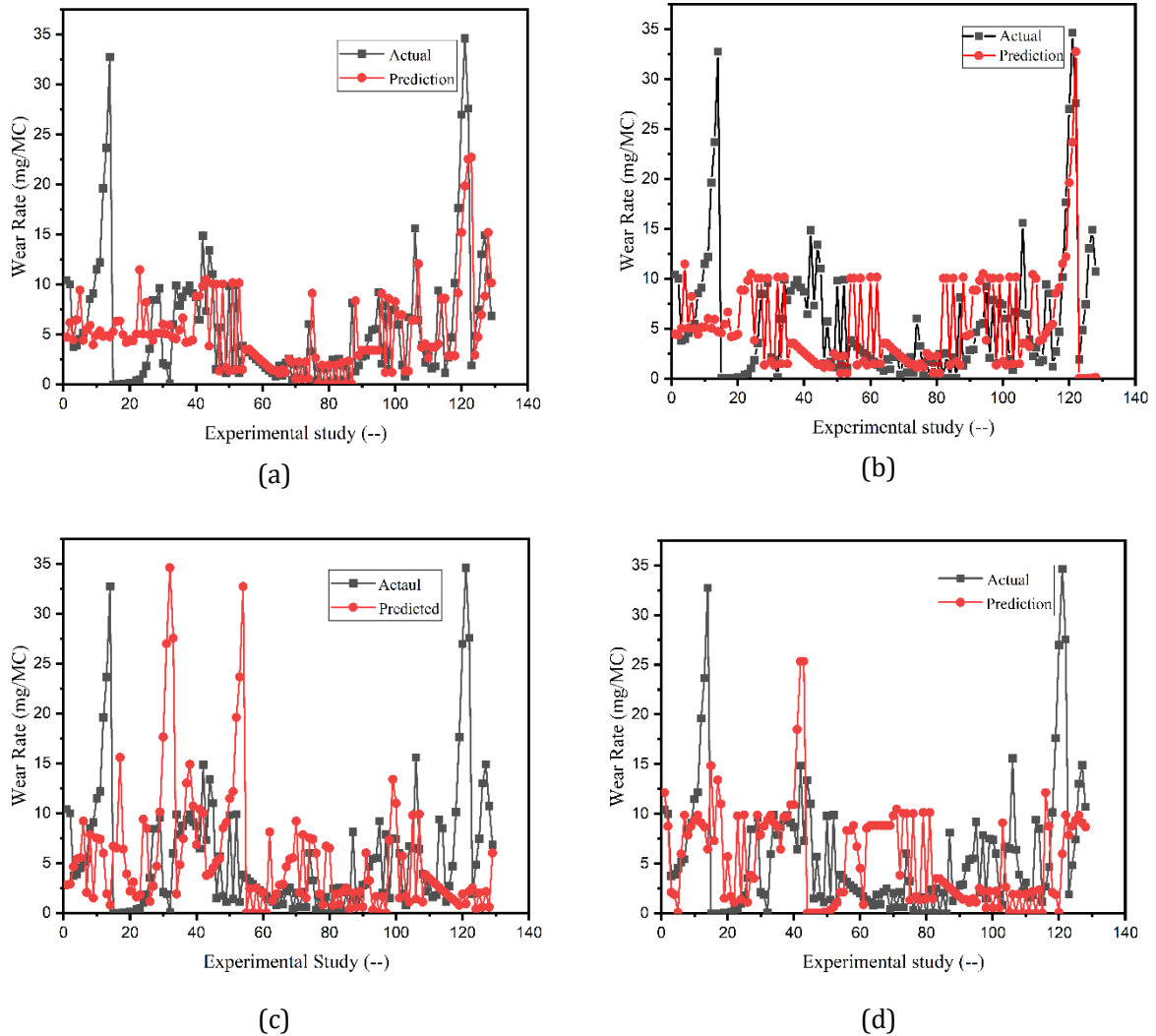


Figure 5. (a) Predicted vs actual wear rate for UHMWPE acetabular cup using RF approach, (b) Predicted vs actual wear rate for UHMWPE acetabular cup using GBM, (c) Predicted vs actual wear rate for UHMWPE acetabular cup using SVM, (d) Predicted vs actual wear rate for UHMWPE acetabular cup using ANN.

Table 3 indicates that for the available experimental dataset, the KNN approach is found to perform outstanding with the highest value of square of correlation coefficient i.e. 0.9, indicating satisfactory performance of KNN model. A graphical comparison between the experimental UHMWPE wear rate mentioned in the literature and the corresponding predicted UHMWPE wear rate using KNN model have been shown in Figure 6 (a) and 6 (b). It is observed from Figure 6 (a) that as UHMWPE wear rate may go beyond 25 mg/MC and the wear rate predictions deviates from their respective experimental values in the range of 2 to 33 %. Probably this behaviour of predictions is due to the availability of a lesser amount of experimental data in the wear rate

values higher than 25 mg/MC. This means the model needs more instances for training to reduce prediction error for wear rate greater than 25mg/MC.

The KNN model predicted the UHMWPE wear rate with a prediction accuracy of 90% as compared to Random Forest (RF) model for different values of surface roughness as shown in Figure 6 (c). The other performance metrics viz. MSE, RMSE, and MAE values for KNN are observed as 3.89, 1.97 and 1.02 respectively, demonstrating high prediction accuracy. In contrast to other ML models, a KNN model utilizes nearby points or instances for its prediction capabilities. As part of the prediction process, KNN always looks for the closest existing instances and calculates the distance between them using Equation (6) which enhances its prediction capability. An average of k closest points, as given by Equation (8), is used to determine the final prediction for the new data point. The KNN model predictions have shown good agreement with experimental data up to Ra of 0.075. Beyond Ra = 0.075. Beyond this value, the KNN model is found to predict the wear rates with relatively lesser accuracy. The model has shown this behaviour mainly due to the availability of less amount of data containing Ra value greater than 0.075. Another possible reason for this kind of behaviour is that the values of statistical parameters should ideally be the same for the data used for training and testing of that particular model which is not in the current case.

In the present study, the K-Nearest Neighbours (KNN) model was identified as the most effective machine learning algorithm for predicting the wear rate of Ultra-High Molecular Weight Polyethylene (UHMWPE) in hip replacement implants. The KNN achieved an  $R^2$  value of 0.9 and a Root Mean Square Error (RMSE) of 1.97, indicating its high accuracy and suitability for precise predictions. Similarly, the referenced study from Borjali et. al. (A Borjali et al., 2019) also highlighted the effectiveness of KNN, where it achieved an  $R^2$  value of 0.85 and a Mean Absolute Error (MAE) of 1.38 mg/MC, further confirming its robustness in predicting UHMWPE wear rates compared to other models such as Linear Regression and Random Forest. The studies underscore the strengths of KNN in capturing complex, non-linear relationships between input features and wear rate, which is crucial for accurate wear predictions in hip implants. However, it also highlights the model's sensitivity to the range of available training data. In both studies, the accuracy of KNN decreased when predicting wear rates outside the bounds of the training data, indicating a dependency on the quality and comprehensiveness of the input dataset. This was reflected in the findings where prediction errors increased for wear rates not adequately represented in the training data.

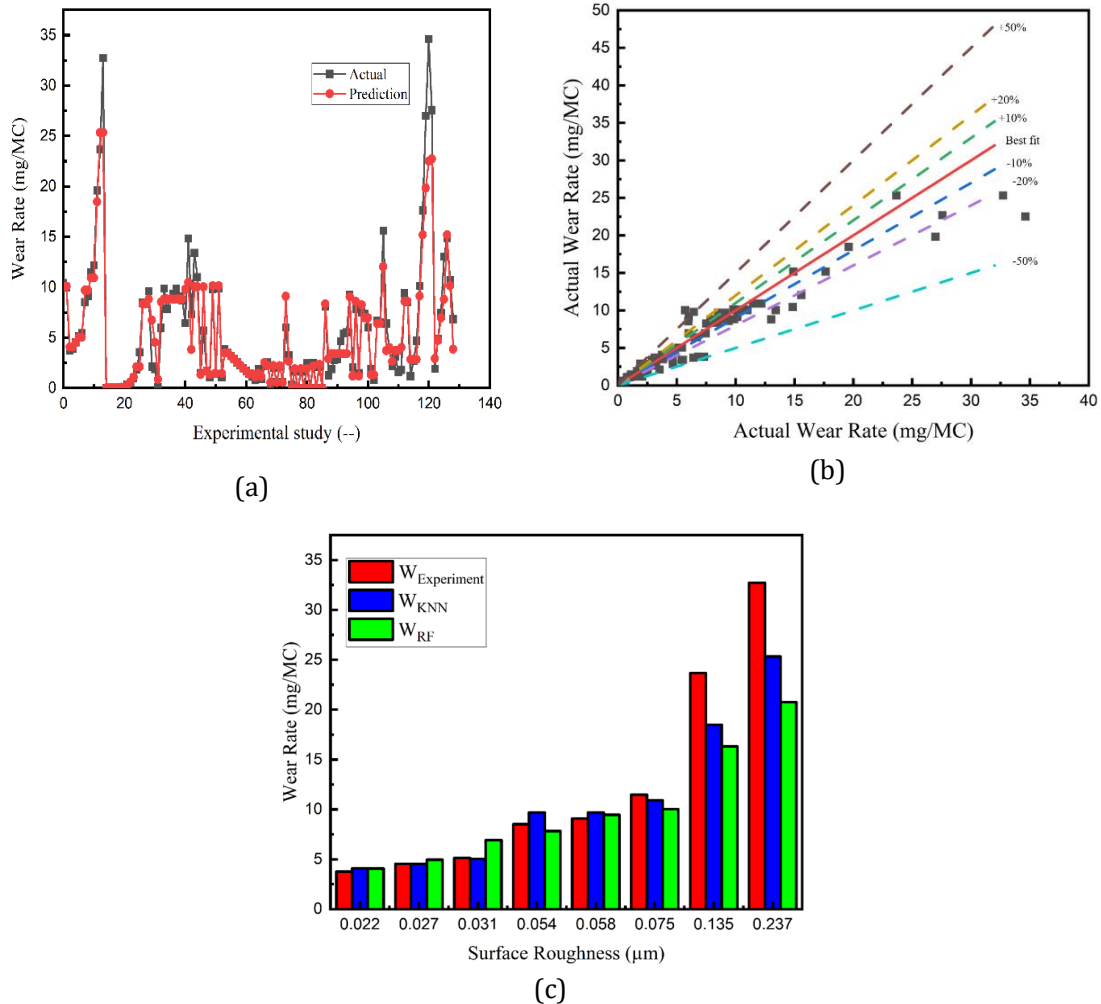


Figure 6. (a) Comparison between Experimental UHMWPE wear rate and the real time predicted wear rate using KNN model, (b) Variation of actual of UHMWPE wear rate from predicted values over a best fit line, (c) Comparison among UHMWPE wear rate obtained from the experimental study, KNN model and Random Forest model for different values of surface roughness.

### 3.3 Parametric Investigation for Wear Rate Evaluation of Hip Joints Using KNN Model Effect Of Radiation Dose on UHMWPE Wear Rate

It can be seen from Table 1 that wear rate depends on radiation dose significantly which is also confirmed by the heat map shown in Figure 4. Therefore, to evaluate a general relationship between wear rate and radiation dose, the values of wear rate at different Radiation doses for a fixed Ra value of 0.054 are evaluated using KNN regression model as shown in Figure 7. An absolute linear pattern of wear rate is observed as radiation dose progresses from 30 kGy to 65 kGy and resulted in progressive and systematic decreases in the rate of wear up to 65 kGy as shown in Figure 7. Beyond 65 kGy, an absolute constant linear pattern is seen, and increasing the radiation dose did not appear to give any additional reduction in the wear rate. These results are

consistent with other scientific works mentioned in the literature (Bracco, Bellare, Bistolfi, & Affatato, 2017). The only difference was observed that only the pattern of obtained results are matched for a given value of Ra. This behaviour was due to difference in test conditions taken during the experimentation. Crosslinking or radiation dose achieved using either gamma or electron beam irradiation, is a common technique for reducing wear. Ionizing radiation produces free radicals, upon removal of hydrogen and breaking chains, which recombine to form the crosslinked structure. It has long been understood that during the walking cycle, the UHMWPE surface of the artificial hip experiences multi-directional sliding against the femoral ball. When sliding perpendicular to the chain orientation direction, this causes a constant reorientation of the polymer chains in the directions of shear stress, resulting in a weakened polymer. By limiting polymer chain orientation from shear stresses, crosslinking creates a material that is more resistant to wear than the untreated polymer.

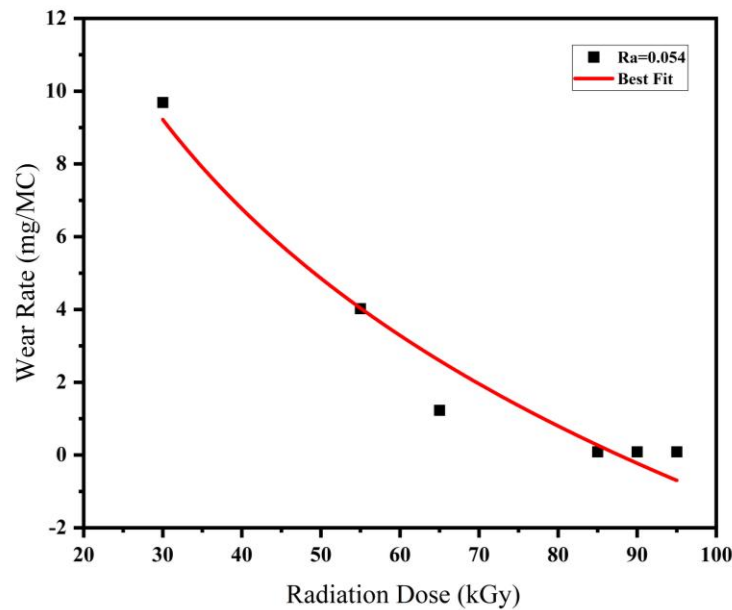


Figure 7: Effect of radiation dose on UHMWPE wear rate and Fitted curve between wear rate and radiation dose.

Further the results obtained above require every time ML based coding. To reduce the time in prediction of wear rates with respect to radiation dose a mathematical model is also fitted as shown in Figure 7.

It is found that the curve fits well with the following Equation (12):

$$W = -2 + 21 \times (0.97)^{R_D} \quad (12)$$

where  $W$  and  $R_D$  are UHMWPE wear rate (mg/MC) and radiation dose (kGy) respectively.

The effect of sliding distance on UHMWPE wear rate for constant values of surface roughness was shown in Figure 8. It can be clearly seen from Figure 8, that UHMWPE wear rate is increasing from 1.59 mg/MC to 7.15 mg/MC as sliding distance varied between 20 to 30 mm/cycle for different surface roughness combinations. It is also noticed that at a lower sliding distances, the difference in the wear rate values for different surface roughness is quite less whereas it is significant for higher values of sliding distances. The cutting action of hard metal asperities and wear debris is reduced under mild sliding conditions compared to severe conditions, and vice versa. Since there is relatively little worn material present at the counterface in the early wear stages, the impacts of the hard metal asperities are more likely to become noticeable at this time. Transferring material onto the counterface fills valleys and smoothes the surface, resulting in less cutting impact from the hard metal. If the sliding distance stabilizes, then wear might decrease (Liu, Ren, Tong, Green, & Arnell, 2002).

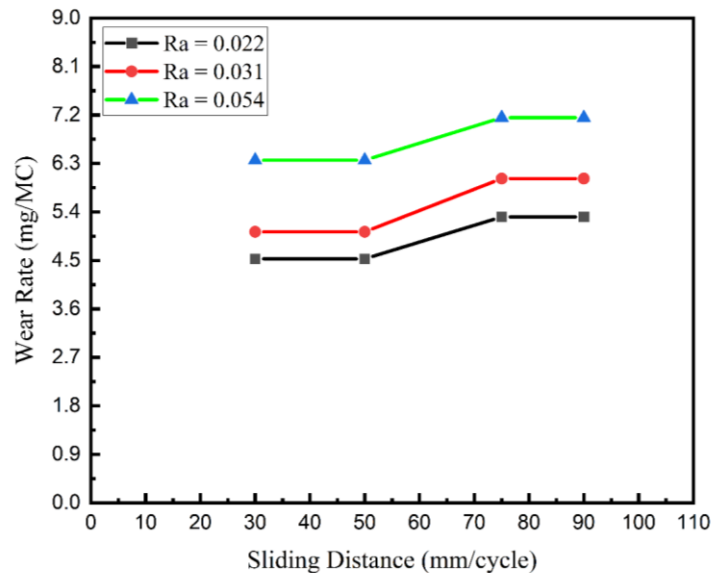


Figure 8: Effect of sliding distance on UHMWPE wear rate.

The machine learning models used in the study, including K-Nearest Neighbors (KNN), Random Forest (RF), and Support Vector Machines (SVM), exhibit varying levels of scalability when applied to larger datasets or real-time applications. The KNN, while effective for smaller datasets, can become computationally intensive with larger datasets due to the need to calculate distances to every data point during predictions. In contrast, models like Random Forest and Gradient Boosting Machines (GBM) are more scalable, handling larger datasets more efficiently through parallelization. For real-time applications, models like SVM and GBM offer quicker predictions once trained, though they require substantial computational resources during training. To ensure scalability in both large-scale and real-time scenarios, optimization of these models or the adoption of hybrid approaches may be necessary to balance accuracy and computational performance.

## CONCLUSIONS

In this current work, UHMWPE wear rates are evaluated with the help of data driven machine learning based models using experimental data reported in the literature. The work is dedicated to check the applicability of machine learning in tribological performance evaluation of THR implants. Out of all machine learning algorithms, the KNN is found to perform outstandingly with the higher value of square of correlation coefficient i.e. 0.9, indicating satisfactory performance of KNN model. The other performance metrics viz. MSE, RMSE and MAE values are also observed as 3.89, 1.97 and 1.02 respectively, demonstrating high prediction accuracy. The KNN model is found to be capturing the exact pattern in data in THRs and thus may be proved as another useful modelling tool for bio-tribological studies. Thus, it can be concluded that KNN modeling can be another alternative to THR implant testing over in-vitro studies to save substantial time and cost. The current study attempts to predict the wear rate of UHMWPE for hip replacement applications using a machine learning algorithm. The available dataset drives the machine learning algorithms. The number of instances and the available experimental data in the dataset is deciding factor for the accuracy and better prediction capability of the particular model. Future studies may incorporate large datasets better to predict UHMWPE wear rate for hip replacement applications. A number of parameters affect this wear and tear which makes the modeling quite complex. For the sake of simplicity and development of initial accurate models, a few parameters for e.g. Cross-shear motion whose experimental data is not available in literature, are omitted in the current work. The effect of cross-shear ratio may also incorporate in future research.

While machine learning models have demonstrated strong predictive capabilities, it is acknowledged that the predictions are not a "perfect" match to the experimental results, likely due to inherent variability in the data and current model limitations. To enhance accuracy, future studies may expand our dataset to include (i) a broader range of wear rates and operating conditions, (ii) biomechanical and patient-specific features, and (iii) may explore hybrid models that combine the strengths of different algorithms. Additionally, we aim to apply our models to real-time monitoring systems for predictive maintenance and validate them through large-scale clinical trials. These future research directions will help refine our method, bringing it closer to perfect alignment with experimental results and improving the durability and reliability of hip replacement implants.

## REFERENCES

- Baykal, D., Siskey, R., Haider, H., Saikko, V., Ahlroos, T., & Kurtz, S. (2014). Advances in tribological testing of artificial joint biomaterials using multidirectional pin-on-disk testers. *Journal of the mechanical behavior of biomedical materials*, 31, 117-134.
- Bini, S. A., Shah, R. F., Bendich, I., Patterson, J. T., Hwang, K. M., & Zaid, M. B. (2019). Machine learning algorithms can use wearable sensor data to accurately predict six-week patient-reported outcome scores following joint replacement in a prospective trial. *The Journal of arthroplasty*, 34(10), 2242-2247.
- Bistolfi, A., & Bellare, A. (2011). The relative effects of radiation crosslinking and type of counterface on the wear resistance of ultrahigh-molecular-weight polyethylene. *Acta biomaterialia*, 7(9), 3398-3403.
- Borjali, A., Chen, A. F., Muratoglu, O. K., Morid, M. A., & Varadarajan, K. M. (2020). Detecting total hip replacement prosthesis design on plain radiographs using deep convolutional neural network. *Journal of Orthopaedic Research*, 38(7), 1465-1471.

- Borjali, A., Monson, K., & Raeymaekers, B. (2019). Predicting the polyethylene wear rate in pin-on-disc experiments in the context of prosthetic hip implants: Deriving a data-driven model using machine learning methods. *Tribology International*, 133, 101-110.
- Bracco, P., Bellare, A., Bistolfi, A., & Affatato, S. (2017). Ultra-high molecular weight polyethylene: influence of the chemical, physical and mechanical properties on the wear behavior. A review. *Materials*, 10(7), 791.
- Bragdon, C. R., O'Connor, D. O., Lowenstein, J. D., Jasty, M., Biggs, S. A., & Harris, W. H. (2001). A new pin-on-disk wear testing method for simulating wear of polyethylene on cobalt-chrome alloy in total hip arthroplasty. *The Journal of arthroplasty*, 16(5), 658-665.
- Couto, M., Vasconcelos, D. P., Sousa, D. M., Sousa, B., Conceição, F., Neto, E., . . . Alves, C. J. (2020). The mechanisms underlying the biological response to wear debris in periprosthetic inflammation. *Frontiers in Materials*, 7, 274.
- Greenbaum, E. S., Burroughs, B. B., Harris, W. H., & Muratoglu, O. K. (2004). Effect of lipid absorption on wear and compressive properties of unirradiated and highly crosslinked UHMWPE: an in vitro experimental model. *Biomaterials*, 25(18), 4479-4484.
- Gul, R. M., McGarry, F. J., Bragdon, C. R., Muratoglu, O. K., & Harris, W. H. (2003). Effect of consolidation on adhesive and abrasive wear of ultra high molecular weight polyethylene. *Biomaterials*, 24(19), 3193-3199.
- Harsha, A., & Joyce, T. J. (2013). Comparative wear tests of ultra-high molecular weight polyethylene and cross-linked polyethylene. *Proceedings of the Institution of Mechanical Engineers, Part H: Journal of Engineering in Medicine*, 227(5), 600-608.
- Hunt, B. J., & Joyce, T. J. (2016). A tribological assessment of ultra high molecular weight polyethylene types GUR 1020 and GUR 1050 for orthopedic applications. *Lubricants*, 4(3), 25.
- Kang, Y.-J., Yoo, J.-I., Cha, Y.-H., Park, C. H., & Kim, J.-T. (2020). Machine learning-based identification of hip arthroplasty designs. *Journal of orthopaedic translation*, 21, 13-17.
- Kenney, C., Dick, S., Lea, J., Liu, J., & Ebraheim, N. A. (2019). A systematic review of the causes of failure of Revision Total Hip Arthroplasty. *Journal of orthopaedics*, 16(5), 393-395.
- Korduba, L., & Wang, A. (2011). The effect of cross-shear on the wear of virgin and highly-crosslinked polyethylene. *Wear*, 271(9-10), 1220-1223.
- Kurtz, S. M., MacDonald, D. W., Kocagöz, S., Tohfafarosh, M., & Baykal, D. (2014). Can pin-on-disk testing be used to assess the wear performance of retrieved UHMWPE components for total joint arthroplasty? *BioMed research international*, 2014.
- Langhorn, J., Borjali, A., Hippensteel, E., Nelson, W., & Raeymaekers, B. (2018). Microtextured CoCrMo alloy for use in metal-on-polyethylene prosthetic joint bearings: Multi-directional wear and corrosion measurements. *Tribology International*, 124, 178-183.
- Laraia, K., Leone, N., MacDonald, R., & Blanchet, T. A. (2006). Effect of water and serum absorption on wear of unirradiated and crosslinked UHMWPE orthopedic bearing materials. *Tribology transactions*, 49(3), 338-346.
- Levy, Y. D., & Ezzet, K. A. (2013). Poor short term outcome with a metal-on-metal total hip arthroplasty. *The Journal of arthroplasty*, 28(7), 1212-1217.
- Liu, C., Ren, L., Tong, J., Green, S., & Arnell, R. (2002). Effects of operating parameters on the lubricated wear behavior of a PA-6/UHMWPE blend: a statistical analysis. *Wear*, 253(7-8), 878-884.
- Mazzucco, D., & Spector, M. (2003). Effects of contact area and stress on the volumetric wear of ultrahigh molecular weight polyethylene. *Wear*, 254(5-6), 514-522.

- Muratoglu, O. K., Merrill, E. W., Bragdon, C. R., O'Connor, D., Hoeffel, D., Burroughs, B., . . . Harris, W. H. (2003). Effect of radiation, heat, and aging on in vitro wear resistance of polyethylene. *Clinical Orthopaedics and Related Research*, 417, 253-262.
- Nakanishi, Y., Nakashima, Y., Fujiwara, Y., Komohara, Y., Takeya, M., Miura, H., & Higaki, H. (2018). Influence of surface profile of Co-28Cr-6Mo alloy on wear behaviour of ultra-high molecular weight polyethylene used in artificial joint. *Tribology International*, 118, 538-546.
- Oral, E., Neils, A., & Muratoglu, O. K. (2015). High vitamin E content, impact resistant UHMWPE blend without loss of wear resistance. *Journal of Biomedical Materials Research Part B: Applied Biomaterials*, 103(4), 790-797.
- Oral, E., Wannomae, K. K., Hawkins, N., Harris, W. H., & Muratoglu, O. K. (2004).  $\alpha$ -Tocopherol-doped irradiated UHMWPE for high fatigue resistance and low wear. *Biomaterials*, 25(24), 5515-5522.
- Pandey, A., Kumar, V., Rawat, A., & Rawal, N. (2023). Prediction of effect of wind speed on air pollution level using machine learning technique. *Chemical Product and Process Modeling*(0).
- Saikko, V. (2017). Effect of contact area on the wear and friction of UHMWPE in circular translation pin-on-disk tests. *Journal of Tribology*, 139(6).
- Saikko, V., Calonius, O., & Keränen, J. (2001). Effect of counterface roughness on the wear of conventional and crosslinked ultrahigh molecular weight polyethylene studied with a multi-directional motion pin-on-disk device. *Journal of Biomedical Materials Research: An Official Journal of The Society for Biomaterials, The Japanese Society for Biomaterials, and The Australian Society for Biomaterials and the Korean Society for Biomaterials*, 57(4), 506-512.
- Saikko, V., Calonius, O., & Keränen, J. (2004). Effect of slide track shape on the wear of ultra-high molecular weight polyethylene in a pin-on-disk wear simulation of total hip prosthesis. *Journal of Biomedical Materials Research Part B: Applied Biomaterials: An Official Journal of The Society for Biomaterials, The Japanese Society for Biomaterials, and The Australian Society for Biomaterials and the Korean Society for Biomaterials*, 69(2), 141-148.
- Saikko, V., Morad, O., & Viitala, R. (2021). Effect of type and temperature of serum lubricant on VEXLPE wear and friction. *Wear*, 470, 203613.
- Saikko, V., Morad, O., & Viitala, R. (2022). Effect of temperature on UHMWPE and VEXLPE friction and wear against CoCr in noncyclic tests. *Wear*, 490, 204190.
- Sawae, Y., Yamamoto, A., & Murakami, T. (2008). Influence of protein and lipid concentration of the test lubricant on the wear of ultra high molecular weight polyethylene. *Tribology International*, 41(7), 648-656.
- Sethi, A., Rawat, A., Srivastava, V., & Sharma, A. (2022). Artificial neural network models for wall parameters on plug-1 flow characteristics through pipelines. *J Eng Res*.
- Shah, R. F., Bini, S. A., Martinez, A. M., Pedoia, V., & Vail, T. P. (2020). Incremental inputs improve the automated detection of implant loosening using machine-learning algorithms. *The Bone & Joint Journal*, 102(6 Supple A), 101-106.
- Shen, G., Fang, F., & Kang, C. (2018). Tribological performance of bioimplants: a comprehensive review. *Nanotechnology and Precision Engineering*, 1(2), 107-122.
- Srivastava, V., Prakash, A., & Rawat, A. (2022). To Predict Frictional Pressure-Drop of Turbulent Flow of Water Through a Uniform Cross-Section Pipe Using an Artificial Neural Network. In *Recent Advances in Applied Mechanics* (pp. 397-412): Springer.
- Turell, M., Wang, A., & Bellare, A. (2003). Quantification of the effect of cross-path motion on the wear rate of ultra-high molecular weight polyethylene. *Wear*, 255(7-12), 1034-1039.

- Wimmer, M., Sah, R., Laurent, M., & Viridi, A. (2013). The effect of bacterial contamination on friction and wear in metal/polyethylene bearings for total joint repair—A case report. *Wear*, 301(1-2), 264-270.
- Yao, J. Q., Blanchet, T. A., Murphy, D. J., & Laurent, M. P. (2003). Effect of fluid absorption on the wear resistance of UHMWPE orthopedic bearing surfaces. *Wear*, 255(7-12), 1113-1120.